

A comparative study of methods for identifying epigenetic aging moderators

Colin Farrell¹, Kalsuda Lapborisuth¹, Chanyue Hu¹, Kyle Pu¹, Sagi Snir², and Matteo Pellegrini^{1,3}

¹Dept. of Molecular, Cell and Developmental Biology;

University of California, Los Angeles, CA 90095, USA;;

²Dept. of Evolutionary Biology, University of Haifa, Israel;

³Corresponding Author, matteop@mcdb.ucla.edu

1

2 Epigenetic clocks, DNA methylation based chronological age prediction models,
3 are commonly employed to study age related biology. The error between the predicted
4 and observed age is often interpreted as a form of biological age acceleration and many
5 studies have measured the impact of environmental and other factors on epigenetic
6 age. Epigenetic clocks are fit using approaches that minimize the error between the
7 predicted and observed chronological age and as a result they reduce the impact of
8 factors that may moderate the relationship between actual and epigenetic age. Here we
9 compare the standard methods used to construct epigenetic clocks to an evolutionary
10 framework of epigenetic aging, the epigenetic pacemaker (EPM) that directly models
11 DNA methylation as a function of a time dependent epigenetic state. We show that
12 the EPM is more sensitive than epigenetic clocks for the detection of factors that
13 moderate the relationship between actual age and epigenetic state (ie epigenetic age).
14 Specifically, we show that the EPM is more sensitive at detecting sex and cell type
15 effects in a large aggregate data set and in an example case study is more sensitive
16 sensitive at detecting age related methylation changes associated with polybrominated
17 biphenyl exposure. Thus we find that the pacemaker provides a more robust framework
18 for the study of factors that impact epigenetic age acceleration than traditional clocks
19 based on linear regression models.

20

21 1 Introduction

22 Epigenetic clocks, accurate age prediction models made using DNA methylation, are
23 promising tools for the study of aging and age related biology. Beyond predicting the
24 age of an individual to within a couple of years, multiple studies have shown that
25 the difference between the observed and expected epigenetic age can be interpreted
26 as a measure of biological age acceleration [1]. Age acceleration observed using the
27 first generation of epigenetic clocks [2, 3] has been associated with a variety of health
28 outcomes including mortality risk[4, 5], cancer risk [6], cardiovascular disease[7] and
29 other negative health outcomes[8–10]. However, as epigenetic clocks become more
30 accurate, epigenetic age acceleration is no longer associated with mortality [11].

31 Epigenetic clocks are generally trained using a regularized regression model. Given
32 an elastic net model of the form $y = \beta X$ the goal of penalized regression is to max-
33 imize the likelihood by reducing the prediction error of the model, $L(\lambda_1, \lambda_2, \beta) =$
34 $|y - X\beta|^2 + \lambda_2|\beta|^2 + |\lambda_1\beta|$. In the case of epigenetic clocks, the likelihood is maximized
35 by minimizing the difference between the observed and predicted age subject to the

36 elastic net penalty, λ_1 and λ_2 . . Methylation sites that increase modeled error but contain biologically meaningful information may be discarded during model fitting. This problem is magnified in the case of epigenetic clocks where the relationship between methylation and time is nonlinear[12].

40 An alternative and complementary approach to studying epigenetic aging is to
41 model how methylation changes for a predetermined collection of sites with respect
42 to time. To this end, we have developed the epigenetic pacemaker (EPM) [13, 14]
43 to model methylation changes with age. Given j individuals and i methylation sites,
44 under the EPM an individual methylation site can be modeled as $\hat{m}_{ij} = m_i^0 + r_i s_j + \epsilon_{ij}$
45 where \hat{m}_{ij} is the observed methylation value, m_i^0 is the initial methylation value, r_i
46 is the rate of change, s_j is the epigenetic state, and ϵ_{ij} is a normally distributed error
47 term. The r_i and m_i^0 are characteristic of the sites across all individuals and the
48 epigenetic state of an individual s_j is set using information from all modeled sites.
49 Given an input matrix $\hat{M} = [\hat{m}_{i,j}]$ the EPM utilizes a fast conditional expectation
50 maximization algorithm to find the optimal values of m_i^0 , r_i , and s_j to minimize the
51 error between the observed and predicted methylation values across a set of sites. This
52 is accomplished by first fitting a linear model per site using age as the initial s_j . The
53 s_j of the modeled samples is then updated to minimize the error between the observed
54 and predicted methylation values. This process is performed iteratively until the
55 reduction in error is below a specified threshold or the maximum number of iterations
56 is reached. Under the EPM, the epigenetic state has a linear relationship with the
57 modeled methylation data, but not necessarily with chronological age. This allows
58 for nonlinear relationships between time and methylation to be modeled without prior
59 knowledge of the underlying form. Every modeled methylation site has a characteristic
60 m_i^0 and r_i that describes the site in relation to other modeled sites and the output
61 epigenetic states. In the current work, we ask whether the EPM formalism can be
62 utilized for the identification of moderators that impact the association between age
63 and epigenetic state (i.e factors that accelerate or decelerate the changes in epigenetic
64 states with time). To this end we extend the EPM model to simulate methylation
65 matrices associated with age and age accelerating phenotypes. We then evaluate the
66 ability of regularized regression and EPM models to detect age acceleration traits that
67 have linear and nonlinear associations with age. Utilizing a large aggregate data set
68 we validate the simulation results and in one illustrative example further assess the
69 ability of both approaches to detect age related methylation changes associated with
70 PBB exposure.

71 2 Results

72 2.1 Simulation of Trait Associated Methylation Matrices

73 Under the EPM the epigenetic state for individual j , S_j , can be interpreted as a
74 form of biological age that represents a weighted sum of aging associated phenotypes
75 $S_j = \sum_{k=1}^n \alpha_k p_{k,j} + \dots + \alpha_k p_{k,j}$. Under this model α_k is the weight for phenotype
76 k and $p_{k,j}$ is the value of phenotype k . Phenotypes may contribute to increased or
77 decreased aging respectively and when considered as a whole contribute to the overall
78 aging rate observed for an individual.

79 As shown in our previous work[12], the relationship between $p_{k,j}$ and time is not
80 necessarily linear. When simulating age associated phenotypes, each phenotype can
81 be represented as $p_{k,j} = Age_j^{\gamma_k} q_{k,j}$, where γ_k is a phenotype specific parameter shared

among all individuals and $q_{j,k}$ represents the magnitude of exposure for a simulated trait and is personal to an individual. The observed phenotype is modeled as an interaction between age and an exposure of varying magnitude among individuals. This formulation is flexible as non-age dependent traits can be easily simulated by setting $\gamma_k = 0$, $p_{k,j} = q_{k,j} = Age_j^0 q_{k,j}$. Individual sites can be described as a linear model where $\hat{m}_{i,j} = m_i^0 + r_i P_{i,j} + \epsilon_{i,j}$. $P_{i,j}$ is a weighted sum of phenotypes influencing the methylation status of an individual site, $P_{i,j} = \sum_{k=1}^n v_1 p_{1,j} + \dots + v_k p_{k,j}$.

To assess the sensitivity of the EPM and penalized regression approaches at detecting moderator of epigenetic aging we simulated a methylation matrix containing linear and nonlinear age associated traits of form $p_{k,j} = Age_j^{\mathcal{N}(0.5,0.01)} q_{k,j}$ and $p_{k,j} = Age_j^{\mathcal{N}(1,0.01)} q_{k,j}$. The trait γ parameter was generated by sampling from a normal distribution $\mathcal{N}(0.5, 0.01)$ to generate traits with varying relationships with time (Figure 1). Samples were simulated by assigning an age from a uniform distribution, $\mathcal{U}(0, 100)$ and setting sample health by sampling from a normal distribution. Sample health is a sample specific metric that influences the magnitude and direction of the simulated age accelerating trait. Simulated traits included a binary phenotype ($P = 0.5$), continuous phenotypes influenced by only age, or by age and sample health (Table 1). The effect, q , of a binary trait was varied from 0.995 to 1.0 over 5 equally spaced intervals. Given a binary trait form of $p_{k,j} = Age_j^{0.5} q_{k,j}$ a 0.001 decrease in q corresponds to a 1 percent decrease in epigenetic state by age 100 relative to samples not assigned the binary trait. Within each interval the standard deviation of the sample health sampling distribution was varied from 0.0 to 0.01 over 5 equally spaced intervals. The simulation was repeated 50 times for each binary, continuous trait combination with 500 simulated samples within each simulation. Additionally, at a binary q of 0.995 the range of continuous traits was expanded over a broader range to assess the model sensitivity for detecting the continuous trait. Five methylation sites for all continuous traits were then simulated and 50 methylation sites for the binary trait. An additional 50 sites were simulated that were equally influenced by a mixture of four continuous traits and the simulated binary trait. The resulting simulation matrix contains 450 methylation sites.

Given a simulation data set, the samples were split randomly in half for model training and testing. EPM and penalized regression models were fit for each simulation training set and epigenetic state and age predictions were made for the testing set. e then fit a regression model where the epigenetic age or state is dependent on the age, square-root of the age, the health status, and binary trait status of the sample ($S_j = Age + \sqrt{Age} + health_j + binary_j$). The square-root of the age is included in the regression model to account for the nonlinear relationship between the simulated age and methylation data.

As the exposure size of the binary trait is decreased from 1.00 to 0.995 the ability to detect the influence of the trait on the epigenetic state and age is improved (Figure 2A and B). At an effect size of 0.995 the estimated effect of the binary trait on the epigenetic state is significant ($\mu = 0.035, \sigma = 0.089$) while the effect on the epigenetic age it is not ($\mu = 0.269, \sigma = 0.282$). At an exposure size of 1.0, where the simulated binary trait has no effect, the distribution of p values for EPM and linear models is randomly distributed. The ability to observe the health effect of the simulated continuous traits improves in both the linear and EPM models as the standard deviation of the sample health sampling distribution is increased (Figure 2 C and D). At an exposure size of 0.002 and 0.0025 the average EPM model is significant ($\mu = 0.0194, \sigma = 0.0436$) while the average linear model is not ($\mu = 0.0607, \sigma = 0.128$). At a continuous trait

131 standard deviation above 0.005 both models produce significant results.

132 **2.2 Universal Blood EPM and Penalized Regression Mod-
133 els**

134 We validated the simulation results using a large aggregate data set composed of
135 Illumina 450k array data[15–27] deposited in the Gene Expression Omnibus[28] (GEO).
136 All methylation array data sets were processed using a unified pipeline from raw array
137 intensity data (IDAT) files using minfi (Aryee et al., 2014). Sex and blood cell type
138 abundance predictions were made for each processed as previously described[29, 30].
139 The aggregate data set contains 6,251 whole blood tissue samples representing 16 GEO
140 series.

141 We trained EPM and penalized regression models using data assembled from four
142 GEO series[31–34] ($n = 1605$) with samples spanning a wide age range (0.01 - 94.0
143 years). The training set was split by predicted sex, within each sex we used stratified
144 sampling by age to select 95% of the samples for model training. The selected samples
145 from each sex were combined ($n = 1524$) and the remaining samples ($n = 81$) left out
146 for model evaluation. Methylation values for all samples were quantile normalized by
147 probe type[2] using the median site methylation values across all training samples for
148 each methylation site. Principal component analysis (PCA) was performed on the cell
149 type abundance estimates using the training data. The trained PCA model was used
150 to predict the cell type PCs for the testing and validation data sets.

151 We fit a penalized regression model to the training matrix as follows. The normal-
152 ized training methylation matrix was first filtered to remove sites with a variance below
153 0.001, resulting in a training matrix with 183,114 sites. A cross validated ($cv = 5$)
154 elastic net model was trained against training sample ages using the filtered methy-
155 lation matrix. The trained model performed well on the training ($R^2 = 0.981$) and
156 testing ($R^2 = 0.940$) data sets (S.Figure 2).

157 In contrast to penalized regression based approaches, site selection for the EPM
158 model is performed outside of model fitting. Methylation sites were selected for model
159 training if the absolute Pearson correlation coefficient between methylation values and
160 age was greater than 0.4 ($n = 16,880$). A per site regression model was fit using
161 the observed methylation value as the dependent variable and age as the explanatory
162 variable. Sites with a mean absolute error (MAE) less than 0.025 between the predicted
163 and observed methylation values were retained for further analysis ($n = 7,013$). An
164 EPM model was fit using these sites (Figure 3A). We then sought to identify subsets of
165 sites that had functionally similar forms between age and methylation. This was done
166 to filter sites that were associated with age by chance and to select clusters of sites with
167 low prediction error. Subsets of sites with similar functional form were identified by
168 clustering sites using affinity propagation [35]) by the euclidean distance between the
169 single site regression model residuals. Cross validated EPM and penalized regression
170 models were trained for all clusters with greater than ten sites ($n = 55$). The cluster
171 EPM models show varying associations between the epigenetic state and age relative
172 to the EPM model fit with all sites initially selected by absolute PCC(Figure 3B).
173 Clusters with an observed EPM and penalized regression MAE less than 6 ($n = 5$)
174 were combined to fit final EPM and penalized regression models. This resembles
175 the simulated methylation matrices where sites with differing functional forms are
176 modeled collectively. The combined cluster EPM and combined cluster regression
177 model performed well on the training and testing data sets (S.Figure 1).

We evaluated the combined cluster EPM, combined cluster penalized regression, and the full penalized regression models against a validation data set consisting of 14 GEO series experiments representing 4,600 whole blood tissue samples. Each model accurately predicted the epigenetic state or epigenetic age of the validation samples (Figure 4). We then fit an ordinary least squares regression model for every validation experiment individually to predict the observed epigenetic age or state using the sample age, the square root of age, cell type PCs, and predicted sex ($S_j = Age + \sqrt{Age} + PC1 + PC2 + PC3 + Sex + Intercept$). If the proportion of female samples to the total number of samples was greater than 0.7 the sex term was dropped from the regression model. Significant cell type PC2 coefficients were observed for all EPM models and the majority of the cluster and full penalized regression models (Figure 5A). Significant cell type PC1 and PC3 coefficients were observed for the majority of the EPM models but not for the cluster or full penalized regression models. Significant sex effects ($p < 0.0038$) were observed for 9, 4, 0 out of 15 models for the EPM, cluster penalized regression, and full penalized regression respectively (Figure 5B).

2.3 Polybrominated Biphenyls Exposure

Polybrominated biphenyls (PBB) were widely used throughout the United States in the 1960's and 1970's for a variety of industrial applications. Widespread PBB exposure occurred in the state of Michigan from the summer of 1973 to later spring of 1974 when an industrial PBB mixture was incorrectly substituted for a nutritional supplement used in livestock feed[36]. PBB is biologically stable and has a slow biological half life; individuals exposed during the initial 1973 - 1974 incident still have detectable PBB in their blood[37]. PBB is an endocrine-disrupting compound and exposure has been linked to numerous adverse health outcomes in Michigan residents such as thyroid dysfunction[38, 39] and various cancers[40, 41]. A study by Curtis et al. showed total PBB exposure is associated with altered DNA methylation at CpG sites enriched for an association with endocrine-related autoimmune disease [42]. Utilizing the publicly available Illumina Methylation EPIC array [43] profiles ($n = 679$), that covered a wide age range (23 - 88 years), we sought to compare the ability of penalized regression and the EPM to detect epigenetic age acceleration associated with PBB exposure.

Briefly, 50% of samples ($n = 339$) were selected for model training using stratified cross validation by age. A cross validated elastic net model was trained using all methylation sites with a site variance above 0.001, ($n = 529, 703$). The trained model performed well on the training and testing data sets ($R^2 = 1.00, R^2 = 0.740, S.Figure2A - B$). EPM sites were selected and models fit as described with the universal blood EPM. Four EPM clusters ($MAE < 6$) were merged for a combined EPM model built using 413 CpG sites. The combined EPM model performed well in training and testing data sets ($R^2 = 0.794, R^2 = 0.812, S.Figure2C - D$). Epigenetic age and epigenetic state predictions were then made for the testing samples using the penalized regression and EPM models.

We then fit an OLS regression model to predict the epigenetic age or state dependent on PBB-153 exposure, h age, the square root of age, cell type PCs, and predicted sex ($S_j = Age + \sqrt{Age} + PC1 + PC2 + PC3 + Sex + PBB - 153 + Intercept$). PBB-153 exposure was highly significant in the EPM regression model ($p = 5.9e - 10$) but not the penalized regression model ($p = 0.141$).

223 3 Discussion

224 A long standing question in the field of epigenetics was whether biomarkers could be
225 trained to predict various traits using methylation measurements. The most successful
226 biomarkers to date have been epigenetic clocks that can accurately predict the age of
227 an individual based on their methylation pattern. These have been shown to be
228 useful for human studies of aging, as well as for animal studies, including mice[44]
229 and dogs[45]. DNA methylation biomarkers are typically constructed using penalized
230 regression approaches. Given a large enough matrix, penalized regression will select
231 sites that minimize the prediction error given a modeled trait. Epigenetic clocks are
232 examples of such models. Beyond predicting actual ages, these models have also been
233 used to measure the influence of external factors on the rates of aging, and multiple
234 studies have shown that the resulting age accelerations (i.e the differences between
235 actual and predicted ages) are significantly associated with multiple factors such as
236 cardiovascular disease[7] and mortality risk[4, 5].

237 While epigenetic clocks have proven to be useful they have significant limitations.
238 Because they are based on linear models, it may be difficult to model aging when the
239 underlying methylation changes are non-linear in time. Moreover, epigenetic clocks
240 are prone to over fitting, and while cross validation schemes are often used to construct
241 robust clocks, they often do not yield accurate estimates for other data sets. Finally,
242 epigenetic clocks are not very interpretable, and highly degenerate, so that it is difficult
243 to extract biological insights from the weights of the models.

244 To overcome some of these limitations, we have previously developed the epigenetic
245 pacemaker formalism. In this approach, rather than building a model for the age,
246 we construct a model for the observed methylation data that depends on age. The
247 advantage of this approach is that this formalism allows us to identify non-linear
248 associations between methylation and age across a lifespan. Moreover, these models
249 tend to be robust to training as they are fit to large methylation matrices rather than
250 age vectors. Finally, the model describes the change in methylation at each site with
251 respect to a time dependent epigenetic state, and therefore all parameters of the model
252 are directly interpretable as either initial values of methylation or rates of change of
253 methylation.

254 Depending on the context, epigenetic clocks are both more and less effective than
255 the EPM. The penalized regression models provide more accurate age predictions
256 ($R^2 = 0.875, 0.911$) than the EPM model ($R^2 = 0.821$), and the model output can
257 be directly compared to the age of a sample. However, because these models are
258 optimized to reduce the error between actual and predicted age, they tend to minimize
259 the effect of extraneous factors on the predicted age. As such, epigenetic clocks are
260 not optimal for identifying external factors that moderate the relations between actual
261 and predicted age. By contrast, the EPM models are not optimized to minimize the
262 difference between predicted and actual age, but rather try to minimize the difference
263 between observed and modeled methylation values. As such, they retain many of
264 the effects that other factors may have on the association between methylation and
265 epigenetic states.

266 In this study we find that while the penalized regression models were more ac-
267 curate for predicting age, the epigenetic state generated by the EPM is significantly
268 impacted by cell type and sex effects in both simulations and real data. We also
269 found that The EPM model generated for individuals exposed to PBB was sensitive
270 to e PBB exposure, which has been linked to negative health outcomes, while the
271 penalized regression epigenetic aging model was not. Additionally, the sensitivity of

272 the EPM to moderators of epigenetic aging has been supported by two recent
273 studies investigating epigenetic aging in marmots[46] and zebras[47]. In the first of
274 these studies, EPM models showed an association between hibernation and slowed
275 epigenetic aging in marmots and in the second an increased epigenetic age associated
276 with zebra inbreeding; no such associations were observed with penalized regression
277 epigenetic age models.

278 Most studies of human epigenetic aging are not motivated by the development of
279 accurate age predictors, since ages are nearly always known in studies, but rather by
280 the discovery of biological aging moderators. The EPM is a more sensitive approach
281 than epigenetic clocks for the detection of factors other than age that influence the
282 epigenome and therefore potentially more useful for discovering moderators of biological
283 aging.

284 4 Methods

285 4.1 Simulation

286 We implemented the simulation framework as a python package with numpy($\geq v1.16.3$)[48]
287 and scikit-learn(v0.24)[49] as dependencies. A simulation run generates a trait-associated
288 methylation matrix and samples are tied to the simulated traits. The simulation pro-
289 cedure is implemented as follows:

- 290 • Traits are initialized that contain the information about the trait relationship
291 with age and a simulated sample phenotype. Given the structure $p_{k,j} = Age_j^{\gamma_k} q_{k,j}$,
292 and k samples and j traits γ is characteristic of the trait. When a sample is
293 passed to a trait, a value of q is generated for the sample by sampling from a
294 normal distribution with a variance characteristic of the simulation trait. Ad-
295 ditionally, each trait can be optionally influenced by a characteristic measure of
296 sample health, h_j . Given, a normally distributed trait $\mathcal{N}(\mu, \sigma^2)$ and a health
297 effect h_j , the sampled distribution for individual j is $\mathcal{N}(\mu + h_j, \sigma^2)$. Continuous
298 and binary traits can be simulated. If a binary trait is simulated, a q other than
299 1 is assigned at a specified probability.
- 300 • Samples are simulated by setting the age by sampling from a uniform distribu-
301 tion over a specified range and by setting a sample health metric h by sampling
302 from a normal distribution centered on zero with a specified variance. Traits
303 passed to a sample simulation object are then set according to the age and health
304 of the sample. Simulated samples retain all the set phenotype information for
305 downstream reference.
- 306 • Methylation sites are simulated by randomly setting the initial methylation
307 value, maximum observable methylation value, the rate of change at the site,
308 and the error observed at each site. Sites are then assigned traits that influence
309 the methylation values at each site.
- 310 • Methylation values are simulated for each site for every individual given the
311 simulated phenotypes with a specified amount of random noise.

312 4.2 Simulation EPM and Penalized Regression Models

313 Simulation data was randomly split in half into training and testing sets. EPM models
314 were fit using the simulated methylation matrix against age. Penalized regression

315 models were fit using scikit-learn(v0.24)[49] ElasticNet (alpha=1, l1_ratio=0.75, and
316 selection=random). All other parameters were set to their default values. Ordinary
317 least squares regression as implemented in statsmodels (0.11.1)[50] was utilized to
318 describe the epigenetic state or age with the following form ($S_j = Age + \sqrt{Age} +$
319 $health_j + binary_j$). Full analysis is found in the EPMSimulation.ipynb supplementary
320 file.

321 4.3 Methylation Array Processing

322 Metadata for Illumina methylation 450K Beadchip methylation array experiments
323 deposited in the Gene Expression Omnibus (GEO) [28] with more than 50 samples
324 were parsed using a custom python tool set. Experiments that were missing methy-
325 lation beadchip array intensity data (IDAT) files, made repeated measurements of
326 the same samples, utilized cultured cells, or assayed cancerous tissues were excluded
327 from further processing. IDAT files were processed using minfi[30] (v1.34.0). Sample
328 IDAT files were processed in batches according to GEO series and Beadchip identi-
329 fication. Methylation values within each batch were normal-exponential normalized
330 using out-of-band probes[51]. Blood cell types counts were estimated using a regres-
331 sion calibration approach[29] and sex predictions were made using the median intensity
332 measurements of the X and Y chromosomes as implemented in minfi[30]. Whole blood
333 array samples were used for downstream analysis if the sample median methylation
334 probe intensity was greater than 10.5 and the difference between the observed and
335 expected median unmethylation probe intensity is less than 0.4, where the expected
336 median unmethylated signal is described by ($y = 0.66x + 3.718$).

337 4.4 Blood EPM and Penalized Regression Models

338 Methylation sites with an absolute Pearson correlation coefficient between methyla-
339 tion values and age greater than 0.40 and 0.45 for the unified whole blood and PBB
340 data sets respectively were initially selected for EPM model training. A linear model
341 was generated using numpy polyfit [48] with age and the independent variable and
342 methylation values as the dependent variable. Mean absolute error (MAE) was calcu-
343 lated as the mean absolute difference between the observed and predicted meth values
344 according to the site linear models. A vector of residuals generated using these models
345 were utilized for clustering by affinity propagation[35]) as implemented in scikit-learn
346 (v0.24)[49] with a random state of 1 and a cluster preference of -2.5. Cross-validated
347 EPM, and penalized regression models for the universal blood analysis, were trained
348 for all clusters containing greater than ten sites. Clusters with an observed EPM and
349 penalized regression MAE less than 6.0 were combined to fit final EPM and regression
350 models.

351 Penalized regression models were fit using scikit-learn(v0.24)[49] ElasticNetCV
352 (cv=5 alpha=1, l1_ratio=0.75, and selection=random). All other parameters were
353 set to their default values. Principal Component Analysis as implemented in scikit-
354 learn was utilized with default parameters to perform PCA on training sample cell type
355 abundances. The trained PCA was utilized to calculate cell type PCs for the testing
356 and validation samples. Ordinary least squares regression as implemented in statsmod-
357 els (0.11.1)[50] was utilized describe the epigenetic state or age with the following form
358 ($S_j = Age + \sqrt{Age} + CellTypePC1 + CellTypePC2 + CellTypePC3 + Sex + Intercept$).
359 Full analysis is found in the EPMUniversalClock.ipynb supplementary file.

360 **4.5 Analysis Environment**

361 Analysis was carried out in a Jupyter[52] analysis environment. Joblib[53], SciPy[54],
362 Matplotlib[55], Seaborn[56], Pandas[57] and TQDM[58] packages were utilized during
363 analysis.

364 **4.6 Supplementary Information and Data Availability**

365 All analysis code used can be found at <https://github.com/NuttyLogic/EPM-ModeratorsOfAging>.
366 The data supporting these findings are openly available at GEO under the series
367 GSE105123, GSE105123, GSE107459, GSE111165, GSE111629, GSE116339, GSE121633,
368 GSE124366, GSE125105, GSE128235, GSE140800, GSE140800, GSE142512, GSE151278,
369 GSE156994, GSE43976, GSE51032, GSE51057, GSE59065, GSE61496, GSE69138,
370 GSE73103, GSE74548, GSE74548, GSE87640, and GSE87648.

References

1. Horvath, S. & Raj, K. DNA methylation-based biomarkers and the epigenetic clock theory of ageing. en. *Nat. Rev. Genet.* **19**, 371–384 (June 2018).
2. Horvath, S. *DNA methylation age of human tissues and cell types* 2013.
3. Hannum, G. *et al.* Genome-wide methylation profiles reveal quantitative views of human aging rates. en. *Mol. Cell* **49**, 359–367 (Jan. 2013).
4. Marioni, R. E. *et al.* DNA methylation age of blood predicts all-cause mortality in later life. en. *Genome Biol.* **16**, 25 (Jan. 2015).
5. Perna, L. *et al.* Epigenetic age acceleration predicts cancer, cardiovascular, and all-cause mortality in a German case cohort 2016.
6. Dugué, P.-A. *et al.* DNA methylation-based biological aging and cancer risk and survival: Pooled analysis of seven prospective studies. en. *Int. J. Cancer* **142**, 1611–1619 (Apr. 2018).
7. Huang, R.-C. *et al.* Epigenetic Age Acceleration in Adolescence Associates With BMI, Inflammation, and Risk Score for Middle Age Cardiovascular Disease. en. *J. Clin. Endocrinol. Metab.* **104**, 3012–3024 (July 2019).
8. Armstrong, N. J. *et al.* Aging, exceptional longevity and comparisons of the Hannum and Horvath epigenetic clocks. en. *Epigenomics* **9**, 689–700 (May 2017).
9. Horvath, S. *et al.* Decreased epigenetic age of PBMCs from Italian semi-supercentenarians and their offspring. en. *Aging* **7**, 1159–1170 (Dec. 2015).
10. Horvath, S. *et al.* Obesity accelerates epigenetic aging of human liver. en. *Proc. Natl. Acad. Sci. U. S. A.* **111**, 15538–15543 (Oct. 2014).
11. Zhang, Q. *et al.* Improved precision of epigenetic clock estimates across tissues and its implication for biological ageing 2019.

12. Snir, S., Farrell, C. & Pellegrini, M. Human epigenetic ageing is logarithmic with time across the entire lifespan. en. *Epigenetics* **14**, 912–926 (Sept. 2019).
13. Snir, S., vonHoldt, B. M. & Pellegrini, M. A Statistical Framework to Identify Deviation from Time Linearity in Epigenetic Aging. en. *PLoS Comput. Biol.* **12**, e1005183 (Nov. 2016).
14. Farrell, C., Snir, S. & Pellegrini, M. The Epigenetic Pacemaker: modeling epigenetic states under an evolutionary framework. en. *Bioinformatics* **36**, 4662–4663 (Nov. 2020).
15. Marabita, F. *et al.* Author Correction: Smoking induces DNA methylation changes in Multiple Sclerosis patients with exposure-response relationship. en. *Sci. Rep.* **8**, 4340 (Mar. 2018).
16. Venthram, N. T. *et al.* Integrative epigenome-wide analysis demonstrates that DNA methylation may mediate genetic risk in inflammatory bowel disease. en. *Nat. Commun.* **7**, 13507 (Nov. 2016).
17. Tan, Q. *et al.* Epigenetic signature of birth weight discordance in adult twins. en. *BMC Genomics* **15**, 1062 (Dec. 2014).
18. Johnson, R. K. *et al.* Longitudinal DNA methylation differences precede type 1 diabetes. en. *Sci. Rep.* **10**, 3721 (Feb. 2020).
19. Voisin, S. *et al.* Many obesity-associated SNPs strongly associate with DNA methylation changes at proximal promoters and enhancers 2015.
20. Soriano-Tárraga, C. *et al.* Epigenome-wide association study identifies TXNIP gene associated with type 2 diabetes mellitus and sustained hyperglycemia. en. *Hum. Mol. Genet.* **25**, 609–619 (Feb. 2016).
21. Dabin, L. *et al.* Altered DNA methylation profiles in blood from patients with sporadic Creutzfeldt-Jakob disease
22. Horvath, S. & Ritz, B. R. Increased epigenetic age and granulocyte counts in the blood of Parkinson's disease patients. en. *Aging* **7**, 1130–1142 (Dec. 2015).
23. Kurushima, Y. *et al.* Epigenetic findings in periodontitis in UK twins: a cross-sectional study 2019.
24. Zannas, A. S. *et al.* Epigenetic upregulation of FKBP5 by aging and stress contributes to NF- κ B-driven inflammation and cardiovascular risk. en. *Proc. Natl. Acad. Sci. U. S. A.* **116**, 11370–11379 (June 2019).
25. Braun, P. R. *et al.* Genome-wide DNA methylation comparison between live human brain and peripheral tissues within individuals. en. *Transl. Psychiatry* **9**, 47 (Jan. 2019).
26. Demetriou, C. A. *et al.* Methylome analysis and epigenetic changes associated with menarcheal age. en. *PLoS One* **8**, e79391 (Nov. 2013).
27. Tserel, L. *et al.* Age-related profiling of DNA methylation in CD8+ T cells reveals changes in immune response and transcriptional regulator genes. en. *Sci. Rep.* **5**, 13107 (Aug. 2015).

28. Barrett, T. *et al.* NCBI GEO: archive for functional genomics data sets—update. en. *Nucleic Acids Res.* **41**, D991–D995 (Nov. 2012).
29. Houseman, E. A. *et al.* DNA methylation arrays as surrogate measures of cell mixture distribution. en. *BMC Bioinformatics* **13**, 86 (May 2012).
30. Aryee, M. J. *et al.* Minfi: a flexible and comprehensive Bioconductor package for the analysis of Infinium DNA methylation microarrays. en. *Bioinformatics* **30**, 1363–1369 (May 2014).
31. Johansson, A., Enroth, S. & Gyllensten, U. Continuous Aging of the Human DNA Methylome Throughout the Human Lifespan. en. *PLoS One* **8**, e67378 (June 2013).
32. Liu, Y. *et al.* Epigenome-wide association data implicate DNA methylation as an intermediary of genetic risk in rheumatoid arthritis 2013.
33. Butcher, D. T. *et al.* CHARGE and Kabuki Syndromes: Gene-Specific DNA Methylation Signatures Identify Epigenetic Mechanisms Linking These Clinically Overlapping Conditions. en. *Am. J. Hum. Genet.* **100**, 773–788 (May 2017).
34. Dámaso, E. *et al.* Comprehensive Constitutional Genetic and Epigenetic Characterization of Lynch-Like Individuals. en. *Cancers* **12** (July 2020).
35. Frey, B. J. & Dueck, D. Clustering by passing messages between data points. en. *Science* **315**, 972–976 (Feb. 2007).
36. Fries, G. F. The PBB episode in Michigan: an overall appraisal. en. *Crit. Rev. Toxicol.* **16**, 105–156 (1985).
37. Safe, S. Polychlorinated biphenyls (PCBs) and polybrominated biphenyls (PBBs): biochemistry, toxicology, and mechanism of action. en. *Crit. Rev. Toxicol.* **13**, 319–395 (1984).
38. Jacobson, M. H. *et al.* Serum Polybrominated Biphenyls (PBBs) and Polychlorinated Biphenyls (PCBs) and Thyroid Function among Michigan Adults Several Decades after the 1973–1974 PBB Contamination of Livestock Feed 2017.
39. Curtis, S. W. *et al.* Thyroid hormone levels associate with exposure to polychlorinated biphenyls and polybrominated biphenyls in adults exposed as children. en. *Environ. Health* **18**, 75 (Aug. 2019).
40. Terrell, M. L., Rosenblatt, K. A., Wirth, J., Cameron, L. L. & Marcus, M. Breast cancer among women in Michigan following exposure to brominated flame retardants. en. *Occup. Environ. Med.* **73**, 564–567 (Aug. 2016).
41. Hoque, A. *et al.* Cancer among a Michigan cohort exposed to polybrominated biphenyls in 1973. en. *Epidemiology* **9**, 373–378 (July 1998).
42. Curtis, S. W. *et al.* Exposure to polybrominated biphenyl (PBB) associates with genome-wide DNA methylation differences in peripheral blood. en. *Epigenetics* **14**, 52–66 (Jan. 2019).

43. Pidsley, R. *et al.* Critical evaluation of the Illumina MethylationEPIC BeadChip microarray for whole-genome DNA methylation profiling. en. *Genome Biol.* **17**, 208 (Oct. 2016).
44. Thompson, M. J. *et al.* A multi-tissue full lifespan epigenetic clock for mice. en. *Aging* **10**, 2832–2854 (Oct. 2018).
45. Thompson, M. J., vonHoldt, B., Horvath, S. & Pellegrini, M. An epigenetic aging clock for dogs and wolves. en. *Aging* **9**, 1055–1068 (Mar. 2017).
46. Pinho, G. M. *et al.* *Hibernation slows epigenetic aging in yellow-bellied marmots* en. Mar. 2021.
47. Larison, B. *et al.* *Epigenetic models predict age and aging in plains zebras and other equids* en. Mar. 2021.
48. Harris, C. R. *et al.* Array programming with NumPy. en. *Nature* **585**, 357–362 (Sept. 2020).
49. Pedregosa, F. *et al.* Scikit-learn: Machine Learning in Python. *J. Mach. Learn. Res.* **12**, 2825–2830 (2011).
50. Seabold, S. & Perktold, J. *Statsmodels: Econometric and statistical modeling with python* in *Proceedings of the 9th Python in Science Conference* **57** (2010), 61.
51. Triche Jr, T. J., Weisenberger, D. J., Van Den Berg, D., Laird, P. W. & Siegmund, K. D. Low-level processing of Illumina Infinium DNA Methylation BeadArrays. en. *Nucleic Acids Res.* **41**, e90 (Apr. 2013).
52. Basu, A. *Reproducible research with jupyter notebooks*
53. Varoquaux, G. & Grisel, O. Joblib: running python function as pipeline jobs. *packages. python. org/joblib* (2009).
54. Virtanen, P. *et al.* SciPy 1.0: fundamental algorithms for scientific computing in Python. *Nat. Methods* (Feb. 2020).
55. Hunter, J. D. *Matplotlib: A 2D Graphics Environment* 2007.
56. Waskom, M. seaborn: statistical data visualization. *J. Open Source Softw.* **6**, 3021 (Apr. 2021).
57. McKinney, W. *Python for Data Analysis: Data Wrangling with Pandas, NumPy, and IPython* en (“O’Reilly Media, Inc.”, Oct. 2012).
58. Da Costa-Luis, C. O. tqdm: A Fast, Extensible Progress Meter for Python and CLI. *JOSS* **4**, 1277 (May 2019).

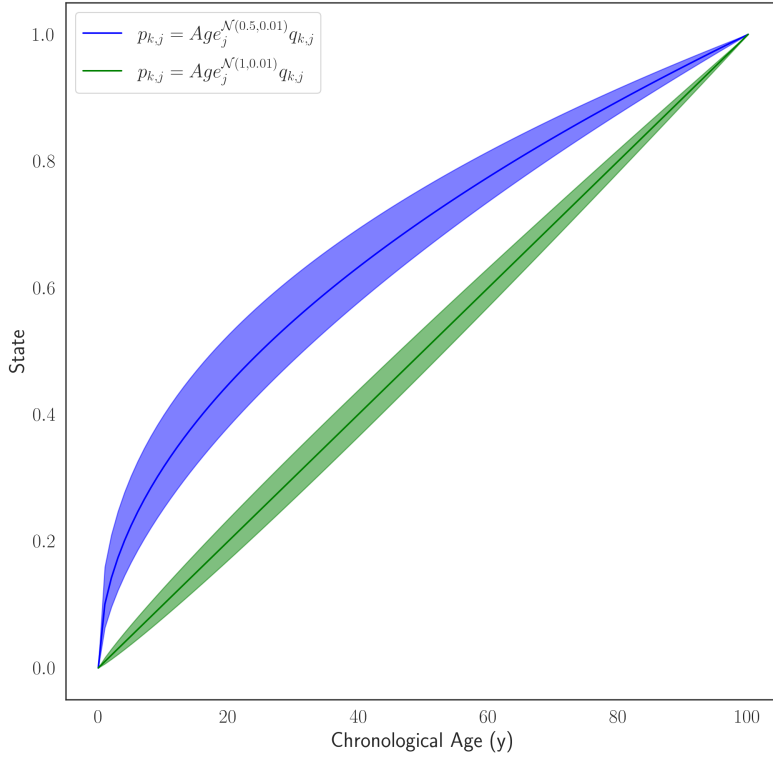


Figure1: Simulated trait forms where the shaded area represent one standard deviation away from the mean γ , given $p_{k,j} = Age_j^{\gamma_k} q_{k,j}$.

Table 1: Simulated Trait Conditions

Trait Form	Beta	Gamma	Gamma Std. Dev.	Sample Effect	Age Only	Generated Phenotypes
Continuous	0.1	$\mathcal{N}(0.5, 0.01)$	0.05	Yes	No	10
Continuous	0.1	$\mathcal{N}(1.0, 0.01)$	0.05	Yes	No	10
Continuous	0.1	$\mathcal{N}(0.5, 0.01)$	0.05	No	Yes	20
Continuous	0.1	$\mathcal{N}(1.0, 0.01)$	0.05	No	Yes	20
Binary ($Pr = 0.5$)	0.1	0.5	0	Yes	No	1

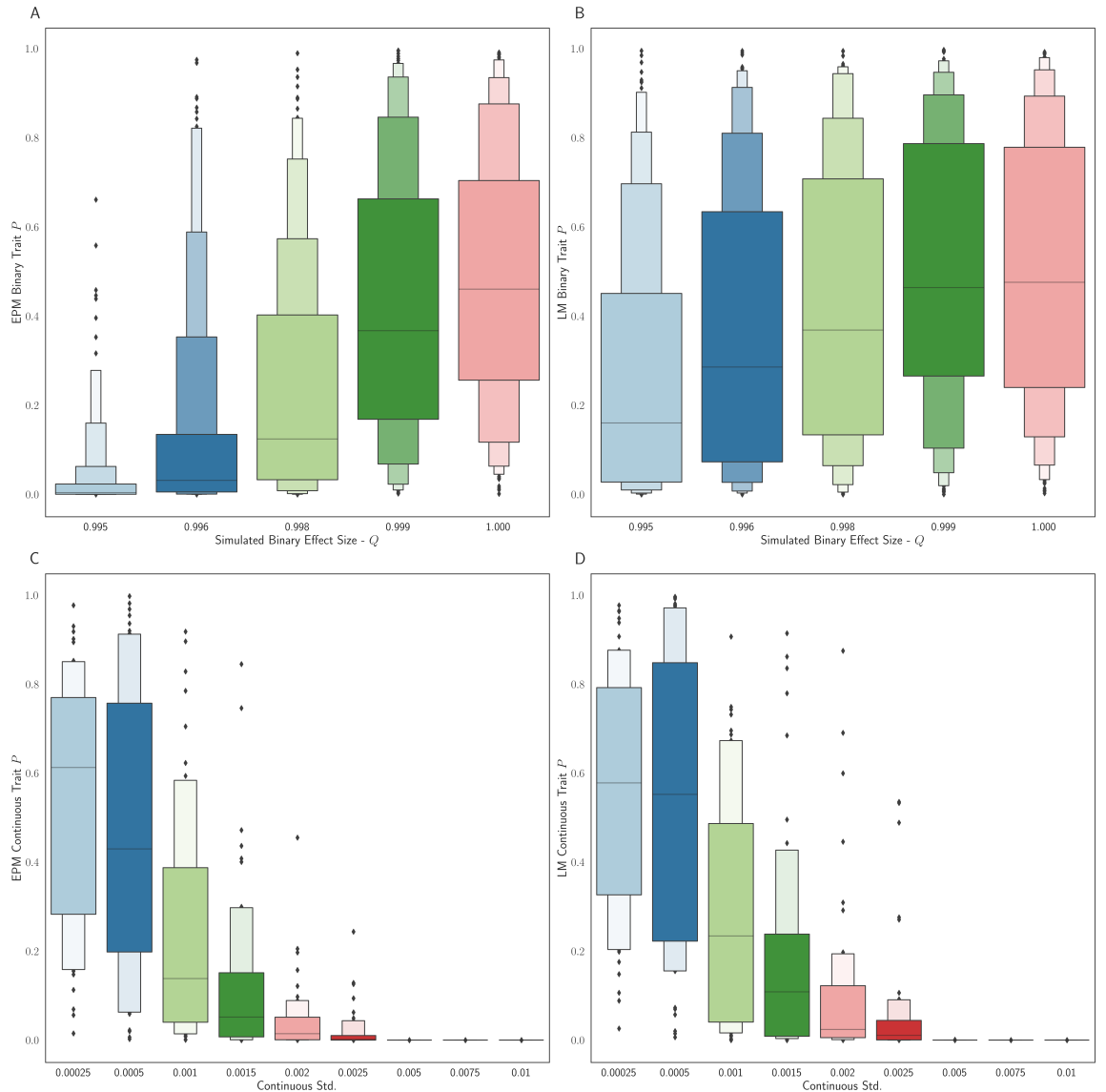


Figure 2: The distribution binary coefficient p-values for **A** EPM and **B** penalized regression models. The distribution of p-values given a simulation health standard deviation for **C** EPM and **D** penalized regression models.

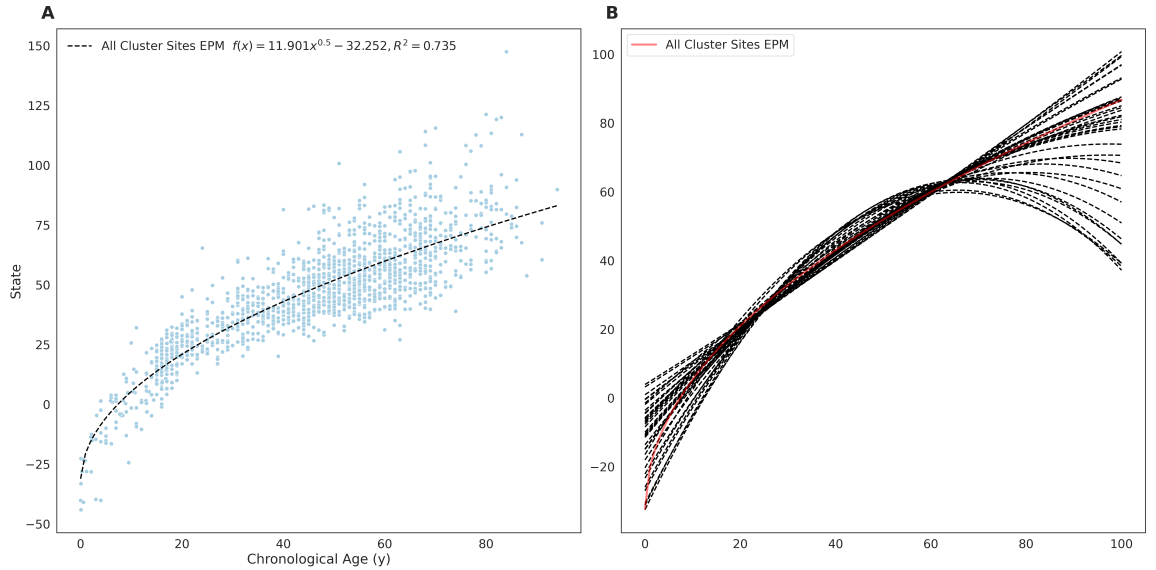


Figure3: **A** EPM model fit with 3832 methylation sites with a MAE below 0.025. **B** The fit trend line for EPM clusters with more than 10 sites and an $R^2 \geq 0.4$.

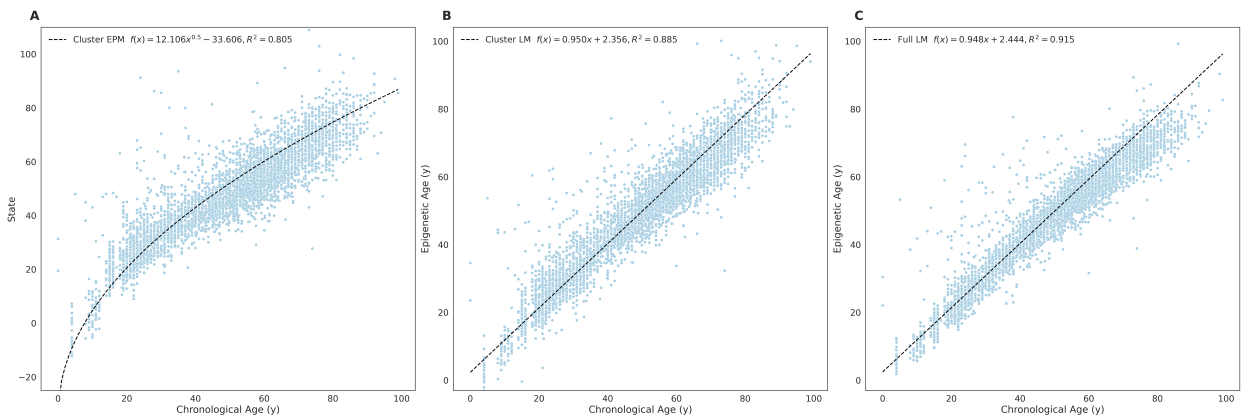


Figure4: Whole blood tissue validation **A** EPM, **B** cluster penalized regression and **C** full penalized regression models.

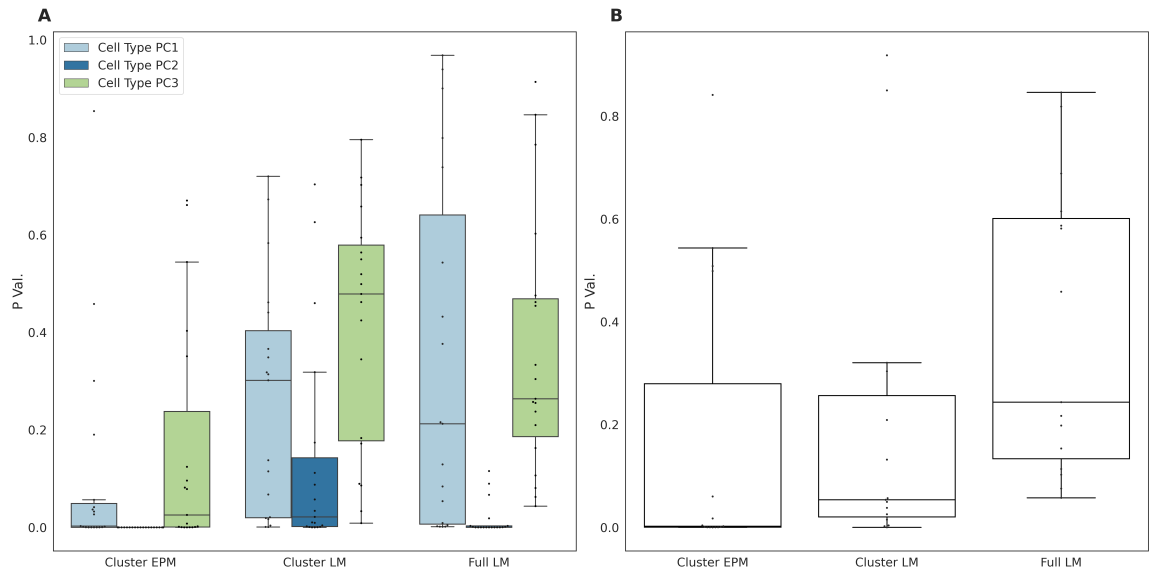
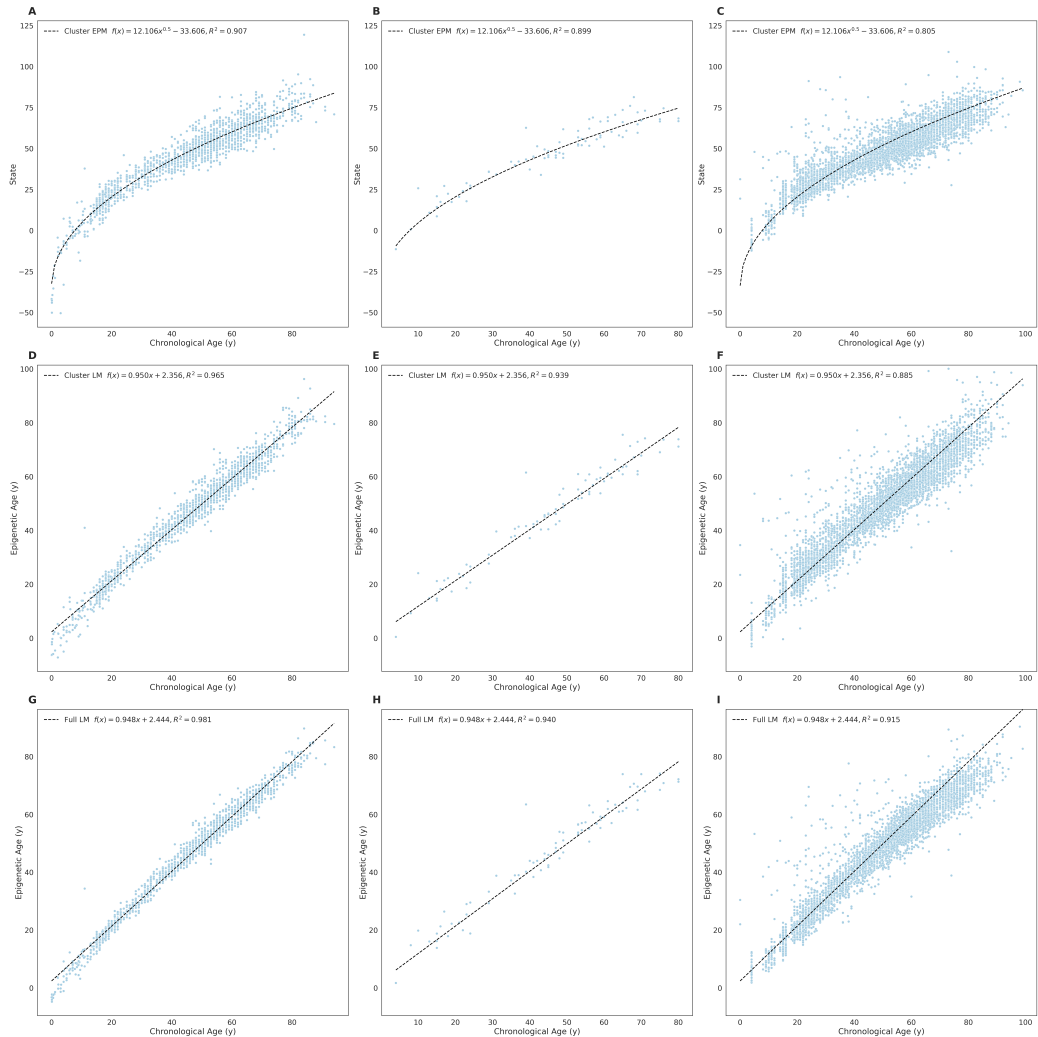
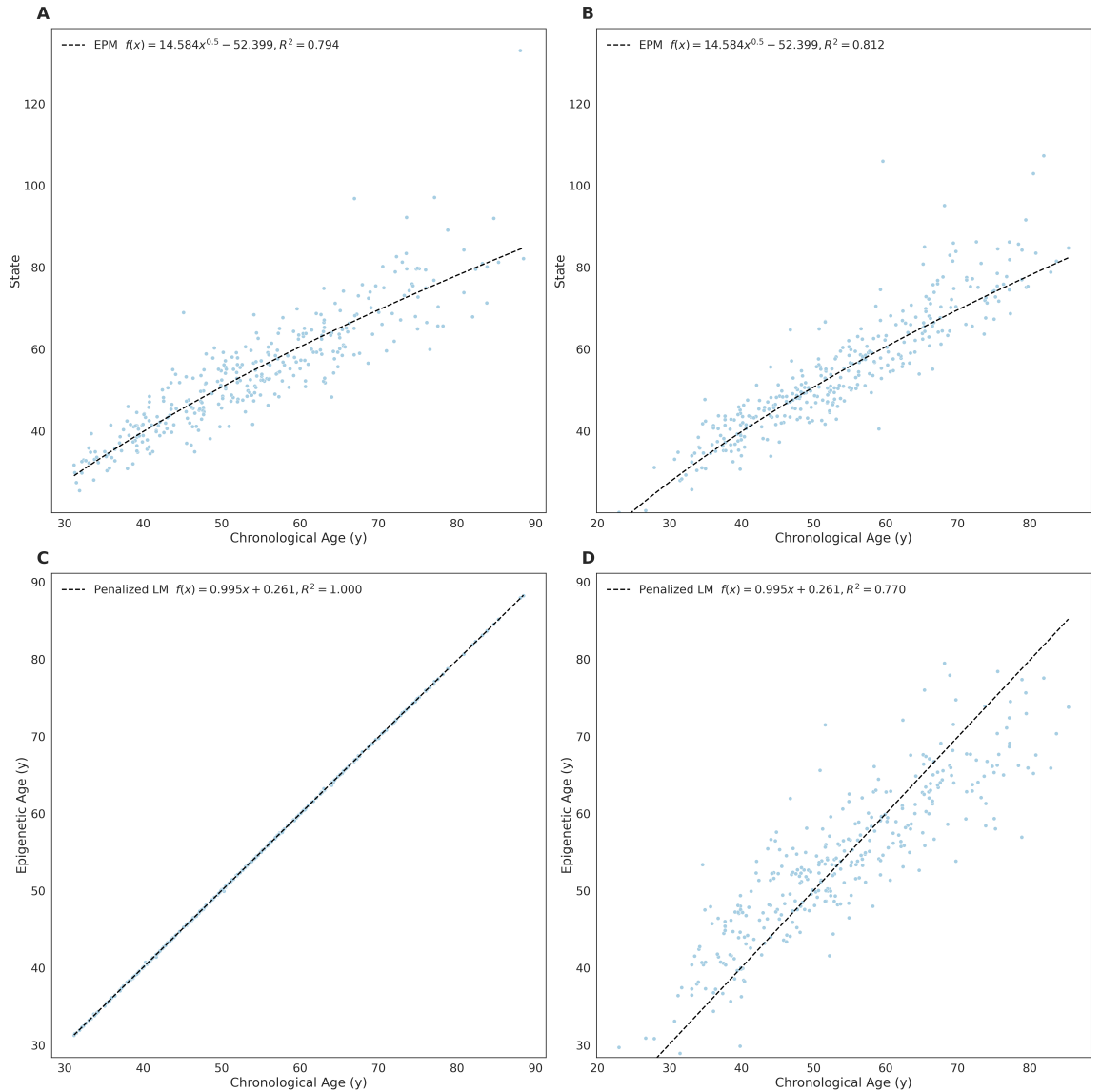


Figure 5: **A** Cell type principal component and **B** predicted sex regression coefficient p-values.



S.Figure1: Universal blood EPM and regression models. **A - C** Train, testing, and validation EPM model. **D-E** Train, testing, and validation cluster penalized regression model. **G-J** Train, testing, and validation full penalized regression model.



S.Figure2: PBB EPM and regression models. **A - B** Train and testing EPM model.
C-D Train and testing penalized regression model.